BJA

British Journal of Anaesthesia, 122 (1): 32–41 (2019)

doi: 10.1016/j.bja.2018.08.009
Advance Access Publication Date: 20 September 2018
Clinical Practice

Abnormal calcium signalling and the caffeine–halothane contracture test

L. Figueroa[1], N. Kraeva[2,3], C. Manno[1], S. Toro[1], E. Ríos[1,*] and S. Riazi[2,3]

[1]Department of Physiology and Biophysics, Rush University Medical Center, Chicago, IL, USA, [2]Malignant Hyperthermia Investigation Unit of the University Health Network, Toronto, ON, Canada and [3]Department of Anaesthesia & Pain Management, Toronto General Hospital, University of Toronto, Toronto, ON, Canada

*Corresponding author. E-mail: erios@rush.edu

This article is accompanied by an editorial: Understanding malignant hyperthermia: each move forward opens our eyes to the distance left to travel by Dirksen et al., *Br J Anesth* 2019:122:8–9, doi: https://doi.org/10.1016/j.bja.2018.10.026.

Abstract

Background: The variable clinical presentation of malignant hyperthermia (MH), a disorder of calcium signalling, hinders its diagnosis and management. Diagnosis relies on the caffeine–halothane contracture test, measuring contraction forces upon exposure of muscle to caffeine or halothane (F_C and F_H, respectively). Patients with above-threshold F_C or F_H are diagnosed as MH susceptible. Many patients test positive to halothane only (termed 'HH'). Our objective was to determine the characteristics of these HH patients, including their clinical symptoms and features of cytosolic Ca^{2+} signalling related to excitation–contraction coupling in myotubes.

Methods: After institutional ethics committee approval, recruited patients undergoing contracture testing at Toronto's MH centre were assigned to three groups: HH, doubly positive (HS), and negative patients (HN). A clinical index was assembled from musculoskeletal symptoms and signs. An analogous calcium index summarised four measures in cultured myotubes: resting $[Ca^{2+}]_{cytosol}$, frequency of spontaneous cytosolic Ca^{2+} events, Ca^{2+} waves, and cell-wide Ca^{2+} spikes after electrical stimulation.

Results: The highest values of both indexes were found in the HH group; the differences in calcium index between HH and the other groups were statistically significant. The principal component analysis confirmed the unique cell-level features of the HH group, and identified elevated resting $[Ca^{2+}]_{cytosol}$ and spontaneous event frequency as the defining HH characteristics.

Conclusions: These findings suggest that HH pathogenesis stems from excess Ca^{2+} leak through sarcoplasmic reticulum channels. This identifies HH as a separate diagnostic group and opens their condition to treatment based on understanding of pathophysiological mechanisms.

Keywords: excitation–contraction coupling; ion channels; malignant hyperthermia; myopathy; skeletal muscle; volatile anaesthetics

Editorial decision: 6 August 2018; **Accepted:** 6 August 2018

Editor's key points

- The diagnosis of malignant hyperthermia relies on the functional analysis of *in vitro* muscle contracture testing, and shows unexplained phenotypic variability.
- The clinical features and cellular calcium signalling properties in muscle biopsies of patients seen in a Canadian malignant hyperthermia testing centre were analysed.
- Patients testing positive to halothane only in the caffeine–halothane contracture test showed more marked clinical features and calcium signalling abnormalities, consistent with a distinct diagnostic group.
- The pathophysiological mechanism and clinical implications of these findings require further study.

Malignant hyperthermia (MH[1,2]; MIM# 145600) is a potentially fatal disorder of excitation–contraction (EC) coupling, a couplonopathy,[3] with underlying alterations of the Ca^{2+} transients that couple action potentials and contractile activation. MH susceptibility (MHS) is usually associated with mutations in *RYR1*, which encodes the Ca^{2+} release channel of the sarcoplasmic reticulum (SR).[4,5] Mutations in the *CACNA1S*[4] and *Stac3* genes[6,7] are also associated with MHS.[8–10]

There are several conditions associated with MHS that can hamper the diagnosis and management.[11] For example, exertional heat stroke[12] and exertional rhabdomyolysis[13,14] associate with the same MH-linked variants.[2,15] The phenotypic variability can lead to additional primary diagnoses, as in 30% of patients with central core disease and 49% of patients with familial idiopathic hyperCKaemia, who are also diagnosed as MH susceptible.[13,15,16]

The caffeine–halothane contracture test (CHCT) or *in vitro* contracture test, which has high sensitivity for the diagnosis of MHS, is performed on at-risk individuals who lack a known causative mutation. The present study focuses on a group of MH-susceptible patients, called 'HH', who reacted normally to caffeine, but were positive to halothane in the CHCT. We address primarily the HH group because we observed more muscle symptoms and signs in the absence of anaesthesia in our cohort compared with other MH-susceptible patients. Because caffeine and halothane enhance SR Ca^{2+} release by different mechanisms,[17–20] the halothane sensitivity of the HH suggests a specific pathogenesis.

Whilst HH patients are MH susceptible, we hypothesise that unique pathophysiological features separate them from the conventional MH-susceptible patients. To test the hypothesis, we undertook the systematic monitoring of Ca^{2+} signals of EC coupling in biopsied muscle cell fragments and in myotubes derived from every biopsy.

Methods

Ethical approval

After approval by the institutional Research Ethics Board of Toronto General Hospital, informed consents were obtained from all patients who underwent CHCT. The consent included sharing of anonymised genomic data for research purposes. The use of biopsies for cell cultures and functional study was approved by the Institutional Review Board of Rush University.

Patients

Our criteria for CHCT included a previous adverse anaesthetic reaction, family history of MH, repeated exercise- or heat-induced rhabdomyolysis, or idiopathic increased serum creatine kinase (hyperCKaemia) and negative genetic testing for MH-causative mutations. Additionally, patients who carried a variant of unknown significance in *RYR1* or *CACNA1S* underwent CHCT. Amongst 121 patients enrolled, 22 had no family or personal history of MH events (detailed in Supplementary Table S3).

Caffeine–halothane contracture test

Susceptibility to MH was diagnosed based on the North American CHCT protocol.[21] Contractile forces (F_C and F_H) were measured on freshly excised muscle bundles with initial twitch responses that met the viability criteria. Bundles were exposed successively to 0.5, 1, 2, 4, 8, and 32 mM caffeine or to halothane 3%. The threshold responses for a positive diagnosis were F_H (in halothane 3%) $\geq$0.7 g and F_C (in 2 mM caffeine) $\geq$0.3. Testing was performed on at least three muscle fascicles per agent; the largest force in each trial determined the diagnosis. Patients were 'MH negative' if the force was below the threshold for both agonists, and 'MH susceptible' if at least one of the exposures exceeded the threshold. We labelled those positive to halothane only as 'HH' and those positive for both agonists as 'HS'.

Molecular genetics

RNA was isolated from blood or muscle, and cDNA synthesis and PCR amplification of the *RYR1* and *CACNA1S* transcripts were performed as published.[22–24] Alternatively, using genomic DNA from blood, we amplified and sequenced the coding regions of all exons plus 20–100 flanking bases in *RYR1*. Sequences were compared with the *RYR1* reference (NM_00540.2 and NC_000019.9) and variants were validated using bioinformatics. To determine whether an unidentified variant segregated with the disease, first- and second-degree relatives were genotyped by Sanger sequencing.

Clinical index

Features related to skeletal muscle involvement were used to compile a clinical index. These included five components: weakness and fatigability (s_1), pain and cramps (s_2), sensitivity to heat or exercise (s_3), CKaemia (s_4), and histopathology (s_5). Based on severity, each was assigned scores between 0 and 2 (normal, mild changes, and severe changes). 'Clinical index' was defined as the equal-weight average of these components, rescaled to the range 0–10. Further details and example provided in Supplementary Table S3.

Cell-level procedures

Biopsied segments of gracilis muscle were shipped to Rush University at 4°C overnight in sterile DMEM-F12 (Gibco, Grand Island, NY, USA) containing antibiotic–antimycotic 1%. Cultures, produced as in Censier and colleagues,[25] were maintained at 37°C in a humid atmosphere containing CO_2 5%. After 8–15 days, cells derived from the explants were transferred in a growth medium to a culture dish for proliferation. Myoblasts were expanded through up to four passages. For optical measurements, myoblasts were reseeded on collagen-coated dishes (MatTek, Ashland, MA, USA). At 70% confluence, the cells were

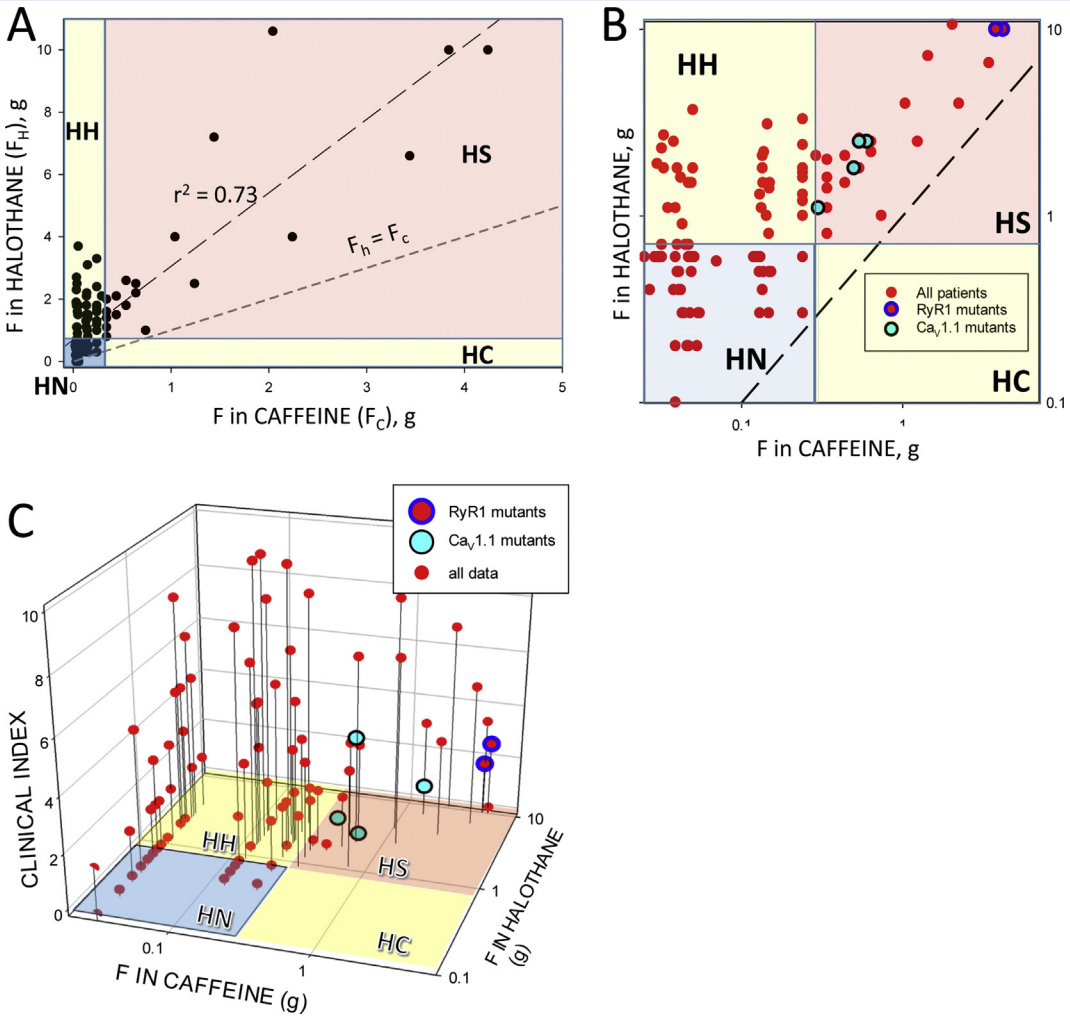

Fig 1. Caffeine-halothane contracture test and clinical index. A, contractile force of muscle strips in response to 2 mM caffeine vs. force in response to 3 vol% halothane. B, same data in logarithmic scales. Results in the blue region are "normal"; patients qualify as HN. The HS region maps forces excessive ("positive") for both caffeine and halothane. Tests in region labeled HH had discrepant results, positive for halothane but not caffeine. No patients had the reciprocal results (the HC region was empty). The correlation between forces induced by caffeine and halothane was high ($r^2 = 0.73$). In both panels the short dashed line represents equal forces in response to both agonists. F_H in HS were generally much greater than in HH. C, Clinical Index, plotted vs. F_C and F_H. The highest values of the index are found in HH patients. The index averages were significantly higher than in HN but the difference between HH and HS was not significant (statistics in Supplemental Table 1). Special symbols identify patients with pathogenic mutations (Supplemental Table 2). In B, the abscissae have a small random number added ($-0.018 > r < 0.018$, smaller than the precision of the measurement) to reduce overlap and provide a better visual depiction of numbers of patients.

switched to a differentiation medium (DMEM-F12 with horse serum 2.5%). Studies were carried out 5–10 days thereafter in myotubes showing a similar degree of maturation. Myoblasts were made from excess biopsied muscle to develop to myotubes or frozen for further propagation. The derivation of cultures was successful in 95 (of 121) patients. Viable myotubes were obtained in up to four passages. The present study used first and second passage cultures.

Cytosolic calcium measurements

Cytosolic Ca^{2+} concentration, $[Ca^{2+}]_{cyto}$, was monitored in myotubes as in Launikonis and colleagues[26] and Zhou and colleagues,[27] by shifted excitation and emission ratioing of indo-1 fluorescence (Invitrogen, Waltham, MA, USA). Imaging was by confocal microscopy (scanner TCS SP2; Leica Microsystems; Buffalo Grove, Illinois, USA), using a 63× 1.2 numerical-aperture water-immersion objective. Calcium transients elicited by field-stimulated action potentials were monitored with fluo-4. $[Ca^{2+}]_{cyto}$ was derived from fluorescence signals and release flux from $[Ca^{2+}]_{cyto}$ as described.[28]

Calcium index

Four measurements, represented as x_j, j=1–4, were made in 20–40 myotubes of multiple cultures from each patient:

resting $[Ca^{2+}]_{cyto}$ (x_1), fraction of myotubes having spontaneous Ca^{2+} sparks or macro-sparks (x_2), fractions having propagated Ca^{2+} waves (x_3), and cell-wide Ca^{2+} spikes after electrical stimulation (x_4). The bin boundaries were chosen so that the x_j in the reference cells (HN) was close to 0, whilst the values from the HS and HH spanned the 0–3 range. The calcium index is the average of the x_j, rescaled to the 0–10 range. Cell-level measurements were performed in 16 patients of each CHCT group.

Solutions

The composition (in mM) of Krebs solution was NaCl 145, KCl 5, $CaCl_2$ 2.6, $MgCl_2$ 1, HEPES 10, and glucose 5.6. For dye loading, cell cultures were in Krebs with 5 μM of indo-1 AM or fluo-4 AM for 35 min at 37°C. The solutions were adjusted to pH 7.2 and 300–320 mOsmol kg^{-1}. The experiments were carried out at 20°C.

Statistics

When distributions satisfied normality tests, averages were compared parametrically; otherwise, properties were compared by non-parametric tests of differences of medians. Measured cell-level variables were subject to principal component analysis (PCA),[29,30] as described in Supplementary methods.

Results

Between January 2013 and December 2017, 121 patients undergoing CHCT at the Malignant Hyperthermia Investigation Unit (Canada) were recruited for this study: 59 (49%) were normal (HN), 21 (17%) were hypersensitive to halothane and caffeine (HS), and 41 (34%) were hypersensitive to halothane only (HH). The mean ages were 37.1, 34.4, and 36.8 yr. 39%, 51%, and 48% of the patients in HN, HS, and HH groups, respectively,were males.

Caffeine–halothane contracture test

Figure 1 shows the relationship between the force generated in response to halothane or caffeine, F_H and F_C, assessed for all patients. The two thresholds divide the space of results in four regions. F_H was on average greatest in the region of doubly positive results, HS. Forces were positively correlated (r^2=0.73), but had a remarkable asymmetry: whilst in many patients, F_H was above the threshold and F_C was not, the reverse was never true. Given that MHS is diagnosed by hypersensitivity to one or both agonists, *the caffeine component of the test was not relevant to MHS diagnosis in this cohort*. The caffeine test instead allowed for the definition of the HH, a group comprising approximately one-third of these patients, with positive response for halothane only.

Clinical index

In Figure 1c, every patient is represented by a symbol at coordinates F_C, F_H, and clinical index. The plot shows that the highest values of clinical index were found in the HH group. The index average was highest in the HH group, but its difference from the HS group is not statistically significant (Supplementary Table S1). A personal or family history of adverse anaesthetic events did not associate with significant differences in clinical index.

Cell-level studies

The first cell-level measure, resting $[Ca^{2+}]_{cyto}$, showed a clear increase in HH and HS myotubes (Table 1). The second measure was frequency of spontaneous Ca^{2+} release, which in myotubes appeared as Ca^{2+} sparks, 'macro-sparks' or waves (Fig 2). Such events were essentially absent in HN myotubes. The other measures quantified the response to an electrical stimulus. That of a normal myotube (Fig 3a) was a fast increase in $[Ca^{2+}]_{cyto}$ usually spanning the whole cell as a result of a brief homogeneous cell-wide release flux (Fig 3b). Trains of stimuli activated HN cells synchronously and Ca^{2+} release terminated immediately after the train (Fig 3c). HH and HS myotubes instead featured moderately frequent Ca^{2+} waves and spikes after an electrical stimulation. Figure 4a displays $[Ca^{2+}]_{cyto}$ in a wave, and Fig 4b shows images of the underlying flux, which emerges from a narrow band that propagates throughout the cell. Figure 4c–e illustrates 'calcium spikes', delayed responses resembling 'triggered activity' of cardiac

Table 1 Calcium index and its components. Column 1 lists resting $[Ca^{2+}]_{cyto}$. Values for individual patients were obtained by averaging measures in 20–40 myotubes per culture. Values listed are equal-weight averages over all patients in the same diagnostic group. Columns 3, 5, and 7 list frequencies, percent ratio of myotubes showing spontaneous or stimulated calcium events, calculated from observations of 20–40 myotubes. The last three rows list difference of medians, used to quantify the probability *P* of the result in the null hypothesis, also listed. The number of cases was 16 for all groups. SEM, standard error of the mean. *Significant difference, $P \leq 0.05$ by Mann–Whitney rank sum test (used for samples that did not meet normality criteria). †Significant difference in two-tailed *t*-test

	1	2	3	4	5	6	7	8	9	10
	$[Ca^{2+}]_{cyto}$ (nM)	P≤	Spontaneous Ca events (%)	P≤	Waves after stimulus (%)	P≤	Spiking after stimulus (%)	P≤	Calcium index	P≤
HS average SEM	111		10		5.7		18		3.3	
	6.1		5.8		2.4		3.7		0.37	
HH average	131		34		4.1		31		5.6	
SEM	8.1		7.8		1.6		5.1		0.40	
HN average	102		1.2		0.7		3.6		1.4	
SEM	3.4		0.9		0.7		1.6		0.24	
HS–HN	3	0.553	0	0.316	0	0.029*	17	0.001*	1.67	0.001*†
HH–HN	20	0.003*†	32	0.001*	0	0.080	28	0.001*	4.17	0.001*
HH–HS	17	0.038*	32	0.003*	0	0.696	11	0.060	2.50	0.001*†

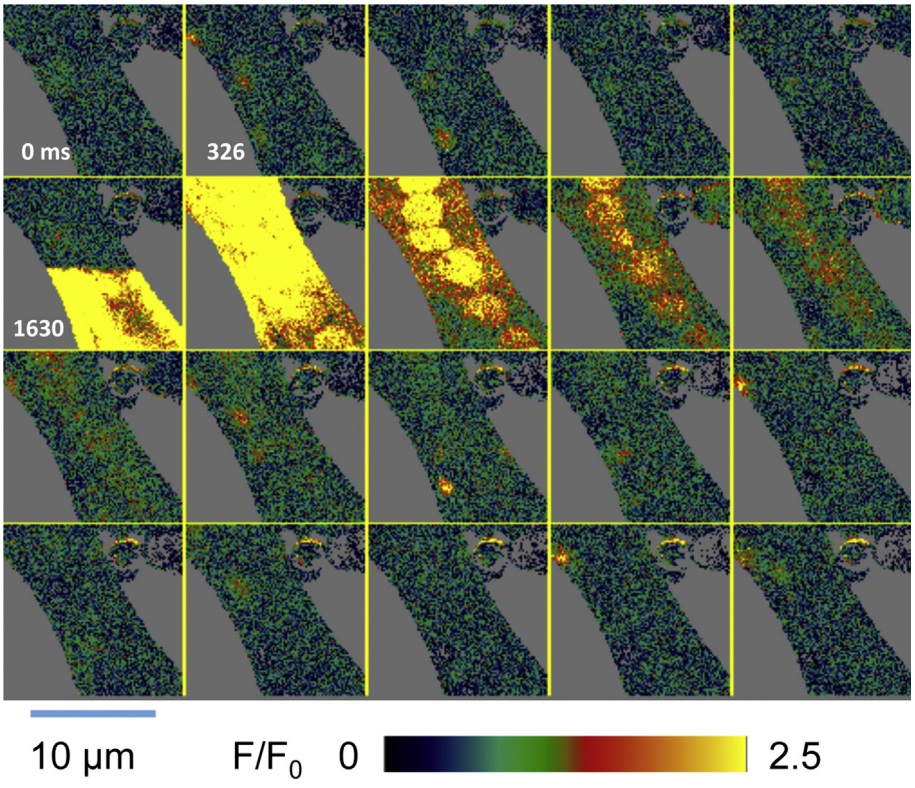

Fig 2. Spontaneous Ca^{2+} events in a myotube from a MH-susceptible patient (Patient #22, diagnosed as HS). Images taken at 326 ms intervals. Spark-like spontaneous events are seen throughout; a propagating wave is first imaged at 1630 ms.

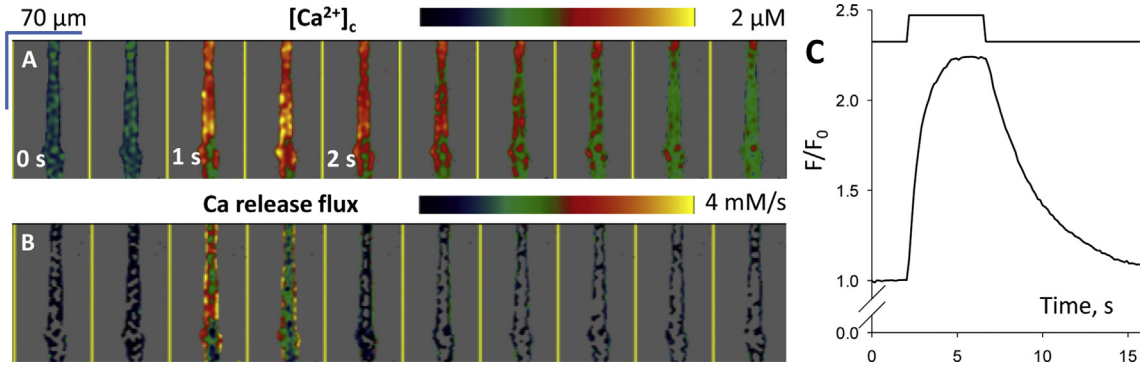

Fig 3. A, Images of $[Ca^{2+}]_{cyto}$ illustrating the normal response to stimulation. B, Ca^{2+} release flux calculated from $[Ca^{2+}]_{cyto}$. Field stimulus applied before 3rd panel. Images taken at 500 ms intervals. The response is immediate, brief and synchronous throughout the cell. (Patient I.D. #9, diagnosed as HN). C, response to a train of pulses (represented schematically at top) in a myotube from another HN patient to show strict association of calcium response to electrical stimulus.

myocytes[31] in their fast rise, occurring nearly simultaneously over wide regions.

By imaging multiple myotubes, we derived the frequencies of cells with spontaneous events, of cells that responded to stimuli with a wave and of cells with spiking (Table 1). The averages of these variables were in all cases significantly greater in the HS and HH groups than in the HN group. They were also greater in the HH than in the HS group, but not significantly for every response type.

These frequencies and the basal $[Ca^{2+}]_{cyto}$ were then combined in a quantifier analogous to the clinical index, the calcium index, plotted in Fig 5a *vs* F_H and F_C for every patient with

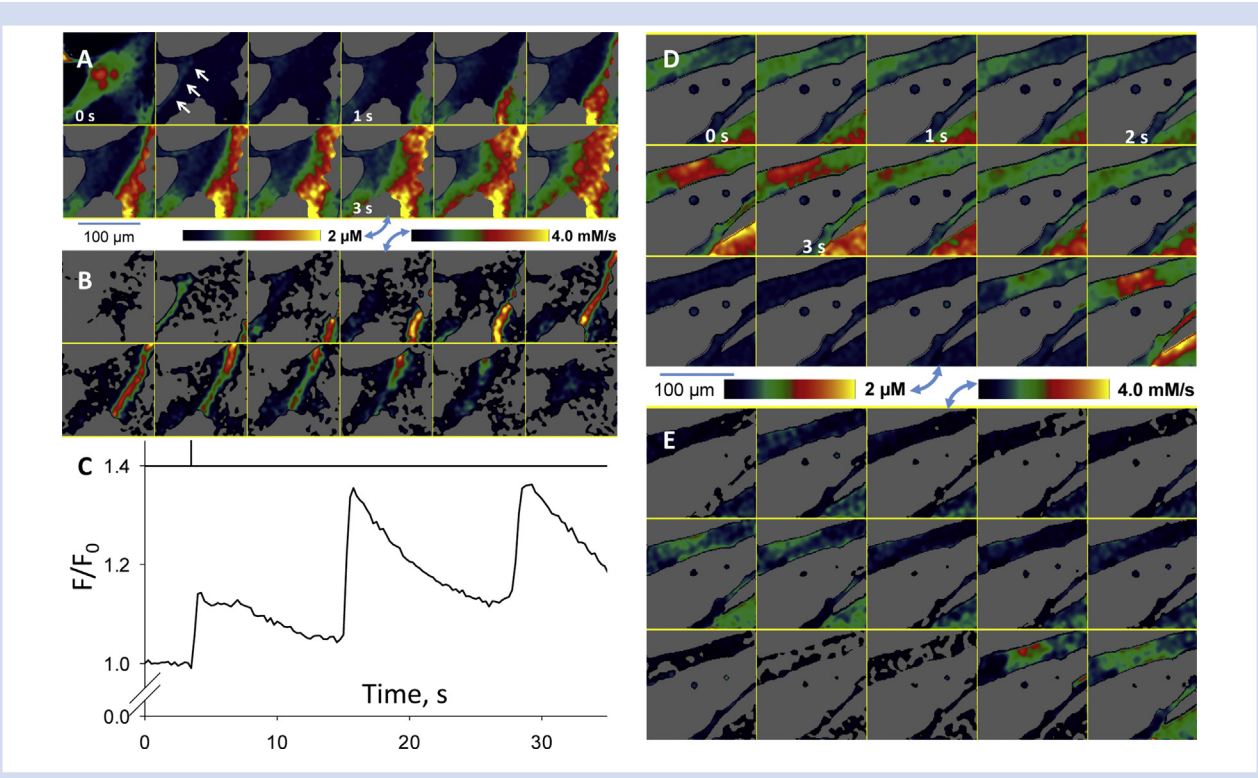

Fig 4. Waves and spikes in response to electrical stimulus. A, cytosolic Ca^{2+} wave and B, Ca^{2+} release flux. The first frame, resting fluorescence at an expanded intensity scale, reveals multiple nuclei. A brief field stimulus was applied at time 0. Arrows in second panel indicate the immediate response to the stimulus, better seen as flux in B. A large increase in $[Ca^{2+}]$ develops later. The Ca^{2+} flux takes the form of a cell-wide wave that propagates right-to-left at 90 μm s^{-1}. Patient #9, diagnosed as HS. C-D, example of "spiking" after a stimulus. C, time course of cell-averaged fluorescence after a single stimulus (trace at top); an immediate response is followed by large fast-rising spikes. Patient #31, diagnosed as HH. D, $[Ca^{2+}]_{cyto}$ transients and E, corresponding Ca^{2+} release flux after a stimulus applied at time 0. Unlike the wave in A, activation of release is fast, repeated, and covers homogeneously large sections of cells. Different myotubes may reactivate at different times. Patient #40, diagnosed as HH.

a completed study. The averages for both the HS and HH groups are significantly greater than for the HN group. As for the clinical index, the average calcium index was highest for the HH group, but in this case, the difference with the HS group was significant (Table 1). When compared separately, three of the index components were significantly higher in the HH than the HN group; the fourth was also higher, but the difference was not statistically significant. Two of the components were significantly higher in the HS than the HN group.

The calcium index is plotted *vs* the clinical index in Fig 5b, with the CHCT diagnostic groups identified.

Both indices mark HH as a group distinct from HN and HS. The moderate correlation between the indices (r^2=0.49) suggests that the clinical and calcium studies provide separate insights into the abnormal HH phenotype.

Multivariate statistical analysis

Calcium index is simply the equal-weight average of scores of four measurements, chosen by their practicality in a large cohort and the assumption that they would reveal distinct relevant aspects of the condition. Recognising some arbitrariness in the procedure, we used PCA as a more objective method (detailed in Supplementary Material). PCA is independent of all clinical knowledge, CHCT included, and transforms the original data ($[Ca^{2+}]_{cyto}$ and three frequencies, represented as x_j) into four 'principal components', c_j. It does so linearly by multiplying the x_j by four sets of four coefficients, one set per component. The components are numbered in decreasing order of their variances, which represent their likely relevance for group separation. The coefficients are listed in Table 2, together with the variances of the respective components. Thus, Component 1 is calculated as

$$c_1 = 0.60x_1 + 0.77x_2 - 0.20x_3 + 0.02x_4 \quad (1)$$

and Component 2 by a similar combination using the coefficients in column 2. A cross plot of the first two principal components is shown in Fig 5c. The HH patients are unequivocally separated from the other groups by principal components.

Variances 1 and 2 together amount to ~90% of the sum of all four variances. This implies that Components 3 and 4 contribute little to the separation of groups; therefore, little is gained by examining these variables. The centres of mass of the three groups (stars in Fig 5c) are close to horizontal, indicating that Component 1 accounts for most of the inter-group variance (the one relevant for classification), whilst that of Component 2 has a large intra-group contribution. The dashed line is the ideal boundary between the normal and altered results according to this analysis. It leaves all but two of the

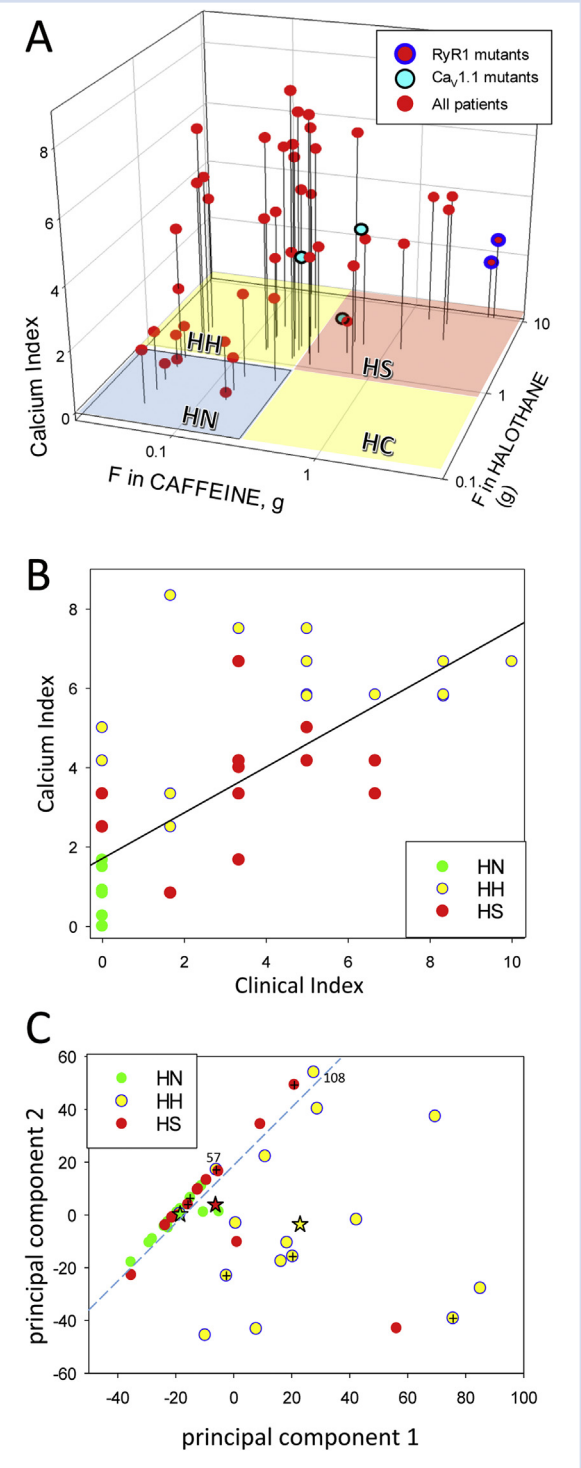

Fig 5. The calcium Index and principal components. A, calcium index, plotted vs. forces in caffeine-halothane contracture test (CHCT). Note that the highest values are found among HH. Special symbols mark the only patients with disease-causing or disease-associated mutations. B, Ca^{2+} and clinical indexes compared. The regression line has a slope of 0.58. $r^2 = 0.49$. B, 2-dimensional principal component analysis. Symbols represent patients, plotted by their principal components 1 and 2. In this plot HH is notably more separated from the other classes than in the graph of panel B. The centers of mass of the group distributions are located by colour-corresponding stars. They align approximately with the axis of principal component 1 (x axis). The dashed line is a tentative border, placed by eye, between a region of normal cell-level phenotype and one of abnormal phenotype. While most HS patients lie on the "normal" side of the line, all but two of the HH patients occupy the "abnormal" region. Two HH outliers are identified by patient ID # next to the symbol. Crosses within symbols identify patients with no personal or family MH history, present in every group.

Table 2 Principal component analysis. Columns 1–4 are the 'eigenvectors' of the linear transformation, sets of coefficients that must be multiplied by the four measured variables of each patient to yield, respectively, principal Components 1–4. The explicit calculation of Component 1 is done by text Equation (1). The 'eigenvalues' are the variances of the transformed data (or principal components), given in absolute terms and as percentages of the total variance. The principal components rank, 1–4, is determined by their variances. Additional details in Supplementary methods and Pearson[29]

Eigenvectors			
1	2	3	4
0.6022	0.6401	−0.0062	0.477
0.7726	−0.6176	−0.0082	−0.1466
−0.2003	−0.4567	0.0351	0.8661
0.0171	0.015	0.9993	−0.0287
Eigenvalues			
1038	623	132	50
56	34	7.2	2.8

HH on the 'abnormal side', in contrast with the HS individuals who fall mostly on the 'normal side' of the line.

Genetic analysis

The results of genetic screening are summarised in Supplementary Table S2. The HH group had no single unifying genetic feature. Only 12% carried *RYR1* variants, all of which are of unknown significance.

Discussion

That all positive MH diagnoses by CHCT of 121 patients were based on an excess F_H implies that the contribution of the caffeine challenge to the diagnosis of MHS was nil in this group. Instead, the absence of reaction to caffeine singled out a group of patients (HH group) who, according to our summary clinical index, were more symptomatic than those hyperreactive to both agonists (HS group). The observation was surprising, given that F_C, the force in reaction to halothane, was, in most HS muscles and on average, greater than in the HH group.

The HH group was heterogeneous. Genetic variants in *RYR1* and *CACNA1S* were present in a minority of HH patients, which indicates that this phenotype was not due *in general* to mutations in these genes, which is consistent with recent reports of difficulties in predicting the pathogenicity of variants

in these genes associated with MH.[32,33] For added insights into pathophysiology, we undertook the cell-level studies. The calcium index, a summary of deviation from normal values in Ca^{2+} handling, was clearly and significantly greater in the HH than in the HS group. A minimal interpretation is that the HH group represents 'non-classical' MHS with a marked disease phenotype in spite of a more limited CHCT abnormality.

PCA exposed more clearly the differential aspects of the HH. A major outcome of the present study is the revelation of greater cell-level functional alterations in the HH group in line with the clinical indications of a more severe phenotype. The outcome is in contrast with the CHCT results, which deviate more strongly and with either agonist in the HS group.

Our choice of cell-level measurements and our interpretation of the results are informed by the distinct modes of action of caffeine and halothane. Caffeine is viewed as an enhancer of the sensitivity of RyR to activation by Ca^{2+},[17,18] separate from the voltage-controlled EC coupling pathway,[20,34] a concept bolstered by the recent identification of a caffeine-binding site within a RyR1 cytosolic hub that also contains sites for Ca^{2+} and activation-promoting ATP.[35,36] Halothane's main effect on RyR1 is instead an increase in sensitivity to activation by voltage,[19] more marked in the RyR1 Y524S MH mouse than in the wild type.[19] This difference in sensitivity, compounded with the increased voltage sensitivity found in the YS and other animal models,[37,38] could be sufficient to explain the catastrophic MH reaction to halothane.[19]

Given their heightened sensitivity to halothane, we envisioned HH cells as having extra sensitivity to depolarisation. This would increase resting Ca^{2+} leak, which will deplete the SR[39] and secondarily increase $[Ca^{2+}]_{cyto}$.[40–43] We also expected HH cells to have more frequent spikes as another manifestation of a putatively increased sensitivity to voltage. In contrast, based on their increased sensitivity to caffeine, we expected HS cells to have enhanced manifestations of calcium-induced calcium release (CICR), namely, spontaneous events and waves after stimulation.

Comparison of these expectations with observations is best done using PCA. The large variance of principal component 1 and the alignment of centres of mass show that this component contains much of the relevant information for separation of the HH group. Component 1 can be viewed as a single-valued summary of the measured variables that is better than the calcium index. Whilst the calcium index gives the same weight to all variables, Component 1 gives high weight to basal $[Ca^{2+}]_{cyto}$ and spontaneous event frequency [Equation (1)].

Elevated resting $[Ca^{2+}]_{cyto}$ is identified as a distinguishing characteristic of HH cells. High $[Ca^{2+}]_{cyto}$ at rest is found in MH models.[44] Our results show that HH cells have a more marked increase than HS cells, suggesting that altered voltage sensitivity, with consequently increased resting leak, is their primary functional defect. The second distinguishing characteristic of HH cells, high spontaneous activity, can be tentatively explained as secondary to the substantial increase in $[Ca^{2+}]_{cyto}$, which will increase the basal activation of RyR and modify its properties in less direct ways. The other measured endpoints, waves and spikes, contribute to principal Components 1 and 2 with small or negative weights, which implies that they do not favour either diagnostic group. Delayed waves and spikes remain opaque in mechanism and significance.

Given the known limitations of work with myotubes, the present measures must be taken as indicators of probable functional properties of the developed myofibre. The patients were heterogeneous in disease aetiology and staging; therefore, group characteristics (e.g. the high value of Component 1 in the HH group) cannot substitute for a detailed study of individual patients.

In conclusion, HH patients are considered MH susceptible; however, they differ from patients with positive responses to both caffeine and halothane in having significant cell-level alterations, manifested in high resting $[Ca^{2+}]_{cyto}$ and spontaneous release activity, features that presumably underlie their altered clinical phenotype. Further understanding of the mechanisms involved requires examination of other variables, including $[Ca^{2+}]_{SR}$, store-operated Ca^{2+} entry, and direct probing of CICR and voltage sensitivity.

Authors' contributions

Study conception: L.F.
Experiment design: E.R., S.R.
Design of cell-level studies: L.F.
Performance of cell-level studies: L.F.
Development of human cultures: L.F.
Production of human cell cultures: S.T.
Development of electrophysiological and imaging techniques: C.M.
Performance of all clinical studies and analyses: N.K., S.R.
Performance of caffeine–halothane contracture test and genetic analyses: N.K., S.R.
Data acquisition: L.F., S.T., E.R., S.R.
Data analysis: L.F., E.R., S.R.
Figure and table preparation: L.F.
Writing of manuscript: E.R., S.R.
All authors contributed to the final version of the text. All authors approved the final manuscript and agreed to be accountable for all aspects of the work.

Acknowledgements

The authors are grateful to F. Zorzato for suggesting the use of multivariate analysis, S. Treves for teaching the culturing of human muscle cells, and E. Tammineni and E. Zvaritch for critical reading of the manuscript.

Declaration of interest

The authors declare that they have no conflicts of interest.

Funding

National Institute of Arthritis and Musculoskeletal and Skin Diseases (R01 AR 071381) to S.R., E.R., and M. Fill (Rush University); National Institute of General Medical Sciences (R01 GM 111254) to E.R., and C.H. Kang (Washington State University).

Appendix A. Supplementary data

Supplementary data related to this article can be found at https://doi.org/10.1016/j.bja.2018.08.009.

References

1. Britt BA. Malignant hyperthermia: a review. In: Schönbaum E, Lomax P, editors. *Thermoregulation: pathology, pharmacology and therapy*. New York: Pergamon Press; 1991. p. 179–292

2. Riazi S, Kraeva N, Hopkins PM. Malignant hyperthermia in the post-genomics era: new perspectives on an old concept. *Anesthesiology* 2018; **128**: 168–80
3. Ríos E, Figueroa L, Manno C, Kraeva N, Riazi S. The couplonopathies: a comparative approach to a class of diseases of skeletal and cardiac muscle. *J Gen Physiol* 2015; **145**: 459–74
4. Rosenberg H, Pollock N, Schiemann A, Bulger T, Stowell K. Malignant hyperthermia: a review. *Orphanet J Rare Dis* 2015; **10**: 93
5. Lillis S, Abbs S, Mueller CR, Muntoni F, Jungbluth H. Clinical utility gene card for: central core disease. *Eur J Hum Genet* 2012; **20**. https://doi.org/10.1038/ejhg.2011.179 [published online 12 October 2011]
6. Stamm DS, Powell CM, Stajich JM, et al. Novel congenital myopathy locus identified in Native American Indians at 12q13.13-14.1. *Neurology* 2008; **71**: 1764–9
7. Horstick EJ, Linsley JW, Dowling JJ, et al. Stac3 is a component of the excitation-contraction coupling machinery and mutated in Native American myopathy. *Nat Commun* 2013; **4**: 1952
8. Robinson RL, Monnier N, Wolz W, et al. A genome wide search for susceptibility loci in three European malignant hyperthermia pedigrees. *Hum Mol Genet* 1997; **6**: 953–61
9. Dainese M, Quarta M, Lyfenko AD, et al. Anesthetic- and heat-induced sudden death in calsequestrin-1-knockout mice. *FASEB J Off Publ Fed Am Soc Exp Biol* 2009; **23**: 1710–20
10. Protasi F, Paolini C, Dainese M. Calsequestrin-1: a new candidate gene for malignant hyperthermia and exertional/environmental heat stroke. *J Physiol* 2009; **587**: 3095–100
11. Maclennan DH, Zvaritch E. Mechanistic models for muscle diseases and disorders originating in the sarcoplasmic reticulum. *Biochim Biophys Acta* 2011; **1813**: 948–64
12. Capacchione JF, Muldoon SM. The relationship between exertional heat illness, exertional rhabdomyolysis, and malignant hyperthermia. *Anesth Analg* 2009; **109**: 1065–9
13. Durham W, Wehrens X, Sood S, Hamilton S. Diseases associated with altered ryanodine receptor activity. In: Carafoli E, Brini M, editors. *Calcium signalling and disease: molecular pathology of calcium*. New York: Springer; 2007. p. 273–321
14. Thomas J, Crowhurst T. Exertional heat stroke, rhabdomyolysis and susceptibility to malignant hyperthermia. *Intern Med J* 2013; **43**: 1035–8
15. Litman RS, Griggs SM, Dowling JJ, Riazi S. Malignant hyperthermia susceptibility and related diseases. *Anesthesiology* 2018; **128**: 159–67
16. Capasso M, De Angelis MV, Di Muzio A, et al. Familial idiopathic hyper-CK-emia: an underrecognized condition. *Muscle Nerve* 2006; **33**: 760–5
17. Rousseau E, Ladine J, Liu QY, Meissner G. Activation of the Ca^{2+} release channel of skeletal muscle sarcoplasmic reticulum by caffeine and related compounds. *Arch Biochem Biophys* 1988; **267**: 75–86
18. Rousseau E, Meissner G. Single cardiac sarcoplasmic reticulum Ca^{2+}-release channel: activation by caffeine. *Am J Physiol* 1989; **256**: H328–33
19. Zullo A, Textor M, Elischer P, et al. Voltage modulates halothane-triggered Ca^{2+} release in malignant hyperthermia-susceptible muscle. *J Gen Physiol* 2018; **150**: 111–25
20. Ríos E. Calcium-induced release of calcium in muscle: 50 years of work and the emerging consensus. *J Gen Physiol* 2018; **150**: 521–37
21. Larach MG. Standardization of the caffeine halothane muscle contracture test. *Anesth Analg* 1989; **69**: 511–5
22. Miller SA, Dykes DD, Polesky HF. A simple salting out procedure for extracting DNA from human nucleated cells. *Nucleic Acids Res* 1988; **16**: 1215
23. Chomczynski P, Sacchi N. The single-step method of RNA isolation by acid guanidinium thiocyanate-phenol-chloroform extraction: twenty-something years on. *Nat Protoc* 2006; **1**: 581–5
24. Kraeva N, Riazi S, Loke J, et al. Ryanodine receptor type 1 gene mutations found in the Canadian malignant hyperthermia population. *Can J Anaesth* 2011; **58**: 504–13
25. Censier K, Urwyler A, Zorzato F, Treves S. Intracellular calcium homeostasis in human primary muscle cells from malignant hyperthermia-susceptible and normal individuals. Effect of overexpression of recombinant wild-type and Arg163Cys mutated ryanodine receptors. *J Clin Invest* 1998; **101**: 1233–42
26. Launikonis BS, Zhou J, Royer L, Shannon TR, Brum G, Ríos E. Confocal imaging of $[Ca^{2+}]$ in cellular organelles by SEER, shifted excitation and emission ratioing of fluorescence. *J Physiol* 2005; **567**: 523–43
27. Zhou J, Yi J, Royer L, et al. A probable role of dihydropyridine receptors in repression of Ca^{2+} sparks demonstrated in cultured mammalian muscle. *Am J Physiol Cell Physiol* 2006; **290**: C539–53
28. Figueroa L, Shkryl VM, Zhou J, et al. Synthetic localized calcium transients directly probe signalling mechanisms in skeletal muscle. *J Physiol* 2012; **590**: 1389–411
29. Pearson K. On lines and planes of closest fit to systems of points in space. *PDF Philos Mag* 1901; **2**: 559–72
30. Abdi H, Williams LJ, Abdi H, Williams LJ. Principal component analysis. *Wiley Interdiscip Rev Comput Stat* 2010; **2**: 433–59
31. Rosen MR. A short, biased history of triggered activity. *Hell J Cardiol HJC Hell Kardiologike Epitheorese* 2009; **50**: 170–8
32. Schiemann AH, Stowell KM. Comparison of pathogenicity prediction tools on missense variants in RYR1 and CACNA1S associated with malignant hyperthermia. *Br J Anaesth* 2016; **117**: 124–8
33. Merritt A, Booms P, Shaw MA, et al. Assessing the pathogenicity of RYR1 variants in malignant hyperthermia. *Br J Anaesth* 2017; **118**: 533–43
34. Shirokova N, Ríos E. Activation of Ca^{2+} release by caffeine and voltage in frog skeletal muscle. *J Physiol* 1996; **493**: 317–39
35. des Georges A, Clarke OB, Zalk R, et al. Structural basis for gating and activation of RyR1. *Cell* 2016; **167**. 145–157.e17
36. Murayama T, Ogawa H, Kurebayashi N, Sakurai T. Molecular basis for Ca^{2+} binding of RyR2 for channel activation and diseases states. *Biophys J* 2018; **114**: 622a
37. Gallant EM, Donaldson SK. Skeletal muscle excitation-contraction coupling. II. Plasmalemma voltage control of intact bundle contractile properties in normal and malignant hyperthermic muscles. *Pflugers Arch* 1989; **414**: 24–30
38. Gallant EM, Lentz LR. Excitation-contraction coupling in pigs heterozygous for malignant hyperthermia. *Am J Physiol* 1992; **262**: C422–6

39. Robin G, Allard B. Major contribution of sarcoplasmic reticulum Ca^{2+} depletion during long-lasting activation of skeletal muscle. *J Gen Physiol* 2013; **141**: 557–65
40. Friel DD, Tsien RW. A caffeine- and ryanodine-sensitive Ca^{2+} store in bullfrog sympathetic neurones modulates effects of Ca^{2+} entry on $[Ca^{2+}]i$. *J Physiol* 1992; **450**: 217–46
41. Ríos E. The cell boundary theorem: a simple law of the control of cytosolic calcium concentration. *J Physiol Sci* 2010; **60**: 81–4
42. Eltit JM, Yang T, Li H, et al. RyR1-mediated Ca^{2+} leak and Ca^{2+} entry determine resting intracellular Ca^{2+} in skeletal myotubes. *J Biol Chem* 2010; **285**: 13781–7
43. Eltit JM, Ding X, Pessah IN, Allen PD, Lopez JR. Nonspecific sarcolemmal cation channels are critical for the pathogenesis of malignant hyperthermia. *FASEB J* 2013; **27**: 991–1000
44. Lopez JR, Alamo LA, Jones DE, et al. $[Ca^{2+}]i$ in muscles of malignant hyperthermia susceptible pigs determined in vivo with Ca^{2+} selective microelectrodes. *Muscle Nerve* 1986; **9**: 85–6

Handling editor: H.C. Hemmings Jr